

Copula-Based Statistical Health Grade System Against Mechanical Faults of Power Transformers

Chao Hu, Pingfeng Wang, Byeng D. Youn, Wook-Ryun Lee, and Joung Taek Yoon

Abstract—A health grade system against mechanical faults of power transformers has been little investigated compared to those for chemical and electrical faults. This paper thus presents a statistical health grade system against mechanical faults in power transformers used in nuclear powerplant sites where the mechanical joints and/or parts are the ones used for constraining transformer cores. Two health metrics—RMS and root mean square deviation of spectral responses at harmonic frequencies—are first defined using vibration signals acquired via insite sensors on 54 power transformers in several nuclear powerplants in 16 months. We then investigate a novel multivariate statistical model, namely copula, to statistically model the populated data of the health metrics. The preliminary study shows that the proposed health metrics and statistical health grade system are feasible to monitor and predict the health condition of the mechanical faults in the power transformers.

Index Terms—Copula, health grade system, health monitoring, power transformer, vibration.

I. INTRODUCTION

THE POWER transformer is one of the most critical power elements in nuclear powerplants and an unexpected transformer breakdown could cause a complete plant shutdown with substantial societal expenses. It is very important to ensure high reliability and maintainability of the transformer during its operation. Investigations of the fault causes have revealed

Manuscript received May 03, 2011; revised March 01, 2012; accepted April 14, 2012. Date of current version September 19, 2012. This work was supported in part by the Power Generation and Electricity Delivery in the Korea Electronics Power Corporation (KEPCO)—Research Institute, funded by the Korean government's Ministry of Knowledge Economy; in part by the National Research Foundation (NRF) of Korea under Grant 2011-0022051, funded by the Korean government; in part by the Basic Research Project of Korea Institute of Machinery and Materials (Project Code SC0830), supported by a grant from the Korean Research Council for Industrial Science and Technology; in part by the Institute of Advanced Machinery and Design at Seoul National University (SNU-IAMD); and in part by a grant from the Energy Technology Development Program of Korea Institute of Energy Technology Evaluation and Planning (KETEP), funded by the Korean government's Ministry of Knowledge Economy. Paper no. TPWRD-00363-2011.

C. Hu was with the Department of Mechanical Engineering, University of Maryland, College Park, MD 20742 USA. He is now with Medtronic, Inc., Minneapolis, MN 55430 USA (e-mail: huchaost@umd.edu).

P. Wang is with the Department of Industrial and Manufacturing Engineering, Wichita State University, Wichita, KS 67260 USA (e-mail: pingfeng.wang@wichita.edu).

B. D. Youn and J. T. Yoon are with the School of Mechanical and Aerospace Engineering, Seoul National University, Seoul 151-744, Korea (e-mail: bdyoun@snu.ac.kr; kaekol@snu.ac.kr).

W.-R. Lee is with the Korea Electric Power Research Institute (KEPRI), Daejeon 305-760, Korea (e-mail: maerong@kepri.re.kr).

Color versions of one or more of the figures in this paper are available online at <http://ieeexplore.ieee.org>.

Digital Object Identifier 10.1109/TPWRD.2012.2202406

TABLE I
BREAKDOWN CLASSIFICATION OF MAIN POWER TRANSFORMERS IN ALL
KOREAN NUCLEAR POWERPLANTS FROM 1978 TO 2002

	Details (Occurrence)	Occurrence	Health Analysis
Electrical failures	<ul style="list-style-type: none"> - Natural disasters (1) - Winding burnouts (2) - Operator mistakes (2) - Accidents in electric power transmission (1) - Mal-operation (4) - Product defects (1) - Manufacturing defect (1) - Product aging (1) 	13	Insulation Diagnosis Test
Chemical failures	<ul style="list-style-type: none"> - Oil burnouts (1) - Impurities in winding (1) - Product defects (1) - Increase of combustible gas (3) 	6	Insulating Oil Analysis
Mechanical failures	<ul style="list-style-type: none"> - Design defect (1) - Manufacturing defect (1) - Part corrosion (3) - Joint failure (3) - Crack, wear failure (5) 	13	N.A.

that mechanical and electric faults are primarily responsible for unexpected breakdowns of the transformers [1]. In total, 32 breakdowns of main power transformers in Korean nuclear powerplants have been reported since 1978. Table I classifies the breakdown causes into three groups (electrical, chemical, and mechanical problems) and ways to manage them [1]. Preventive health management for power transformers has been developed and implemented mainly for chemical and electrical faults. Although mechanical failures are responsible for about 40% of the transformer breakdowns, the nonexistence of generic health metrics or a health grade system makes it difficult to perform preventive maintenance actions for mechanical faults in a timely manner and only corrective maintenance has been employed.

In the literature, substantial research has been carried out for the health monitoring and diagnosis of power transformers. An extensive review of health monitoring and diagnosis methods of power transformers was provided in [2] with a focus on all types of transformer failure causes, and in [3] and [4] with a focus on insulation deterioration. Techniques commonly used for health monitoring of power transformers can be summarized as: 1) online partial-discharge (PD) analysis [5]; 2) dissolved gas analysis (DGA) [6]; 3) frequency-response analysis

(FRA) [7]; 4) moisture-in-oil analysis [8]; 5) oil temperature analysis [1], [9]; 6) winding temperature analysis [10]; 7) load current and voltage analysis [11]; and 8) online power factor analysis [12]. We note that the usage of the vibration signals in monitoring the transformer health has been quite limited. The transformer vibration generated by the core and windings propagates through the transformer oil to the transformer walls where vibration sensors can be placed for vibration measurements [13]–[16]. Bartoletti *et al.* transformed measured acoustic and vibration signals into a frequency domain and suggested a few metrics that could represent the health status of transformers [13]. Ji *et al.* acquired the fundamental frequency component of the core vibration signal as essential features to monitor and assess the transformer health condition [14]. García *et al.* proposed a tank vibration model to detect the winding deformations in power transformers [15] and conducted the experimental verification of the proposed model under different operating conditions and in the presence of winding deformation [16].

Once sensory data are acquired through the health monitoring, the data must be carefully analyzed for health diagnosis in order to identify and classify failures modes. Artificial-intelligence (AI) techniques for pattern recognition have been prevailing for this purpose. Among a wide variety of AI techniques, artificial neural networks (ANNs) have been most widely used in the research dealing with transformer health diagnosis [17], [18]. Despite the good accuracy reported in the literature, the use of ANNs is limited by the intrinsic shortcomings including the danger of overfitting, the need for a large quantity of training data, and numerical instability. In addition to ANNs, the fuzzy logic [19], [20] and expert systems [21], [22] were also developed for transformer health diagnosis. These two approaches take advantage of human expertise to enhance the reliability and effectiveness of health diagnosis systems. Recently, the support vector machine (SVM) has been receiving growing attention with remarkable diagnosis results [23], [24]. The SVM, which employs the structural risk minimization principle, achieves better generalization performance than ANNs employing the traditional empirical risk minimization principle, especially in cases of a small quantity of training data [25].

The status of research on prognostics and health management (PHM) of a power transformer can be summarized as follows.

- 1) Most health monitoring works for power transformers are focused on chemical and electrical failures, but very little on mechanical failures.
- 2) Power transformer oil, gas, and temperatures have been widely used for health monitoring and diagnosis of power transformers. In contrast, the vibration signal has seldom been used for PHM in power transformer applications.
- 3) The PHM studies for power transformers currently stay at the level of monitoring and diagnosis only, with few works on the health prognostics and remaining useful life (RUL) prediction.

This summary suggests the need to construct a health-management database, to formulate a health grade system against mechanical faults, and to investigate the health prognostics for power transformers. To this end, this study presents a

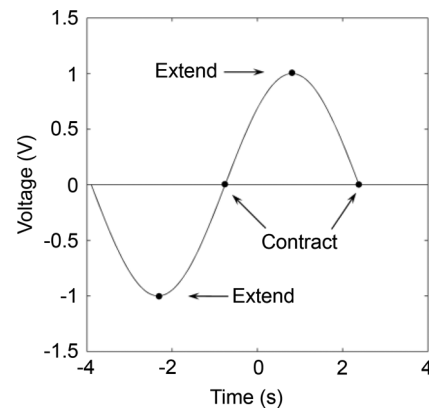


Fig. 1. Magnetostriction in the transformer.

copula-based statistical health grade system against mechanical faults of power transformers. The rest of this paper is organized as follows: Section II introduces the collection and preprocessing of the vibration data for power transformer health monitoring; Section III presents the developed copula-based statistical health grade system for power transformer health monitoring and prognostics against mechanical faults. Section IV provides a discussion of the proposed work followed by the conclusion in Section V.

II. DATA ACQUISITION AND PREPROCESSING

Failures of mechanical joints and/or other parts of power transformers can be detected by analyzing the mechanical vibration properly. This section discusses the fundamentals of transformer vibration, measurement procedures, and data preprocessing.

A. Fundamentals of Transformer Vibration

Power transformer vibrations are primarily generated by the magnetostriction and electrodynamic forces acting on the core and windings during the operation. The vibration of the core and windings propagates through the transformer oil to the transformer walls where vibration sensors can be placed for vibration measurements. The sensors cannot be placed onto the joints because of the transformer oil and magnetic and electric fields that can distort sensory signals. This subsection gives a brief review of the fundamental physics explaining vibrations in the transformer. Various vibration sources exist inside a transformer, contributing to tank vibration. The transformer vibration mainly consists of the core vibration originating from magnetostriction and the winding vibration caused by electrodynamic forces resulting from the interaction of the current in a winding with leakage flux [15]. Other vibration sources include the characteristic acoustic wave produced by the tap changer and periodic vibrations generated by the elements of the cooling system (i.e., oil pumps and fans).

Alternating current (ac) with a constant frequency in power transformers forms a magnetic field in the transformer core. The magnetic field changes the shape of ferromagnetic materials and produces mechanical vibration in the transformer. This phenomenon is called “magnetostriction.” As shown in Fig. 1, one cycle of the ac yields two peaks in the magnetic field. Assume that an

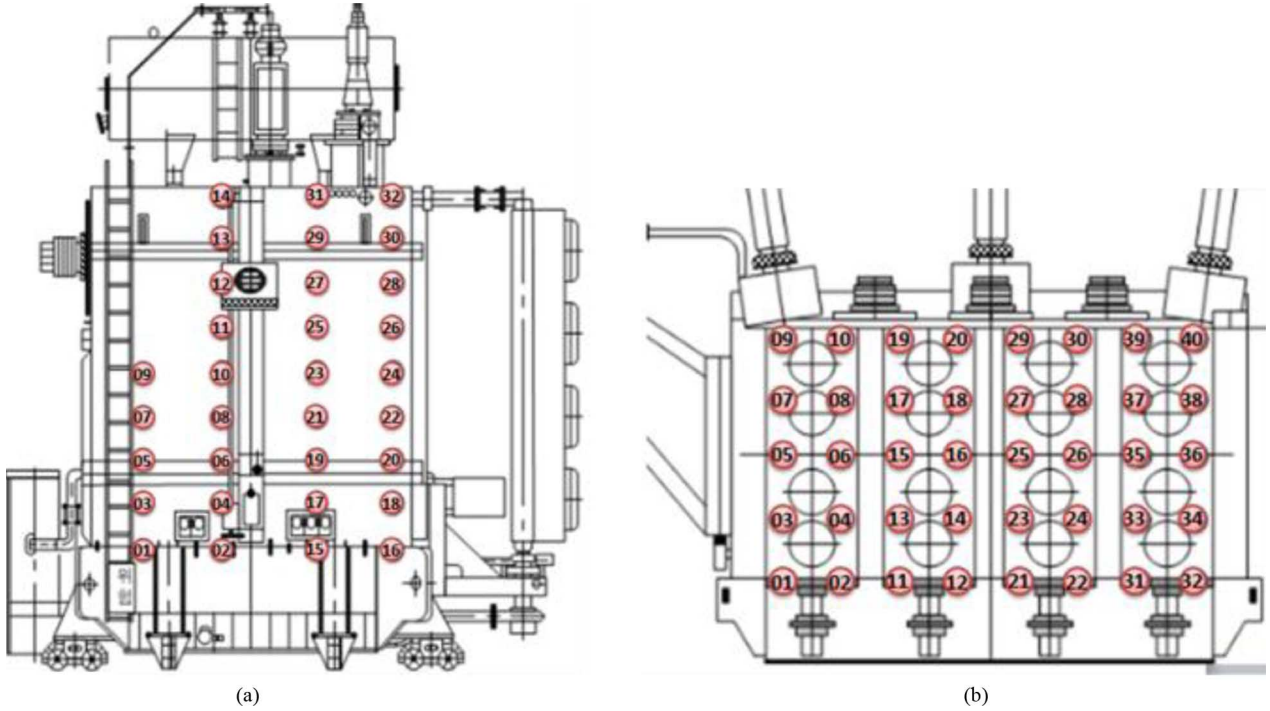


Fig. 2. Sensor locations (marked by red circles with numbers) on the main transformers. (a) Single-phase main transformer. (b) Triple-phase main transformer.

ac source with the amplitude U_0 and frequency f is applied to the drive and that the amplitude is less than or just sufficient to saturate the core. Then, the core vibration acceleration caused by magnetostriction can be expressed as [14]

$$a_c \propto U_0^2 \cos^2 4\pi ft. \quad (1)$$

We can observe from (1) that the magnitude of core vibration exhibits a linear relationship with the square of the ac amplitude. Furthermore, the fundamental frequency of the core vibration is twice that of the ac frequency, as we can also observe in Fig. 1.

Winding vibrations are caused by electrodynamic forces resulting from the interaction of the current in a winding with leakage flux [14]. These forces F_W are proportional to the square of the load current I , expressed as

$$F_W \propto I^2. \quad (2)$$

Since the electromagnetic forces F_W are proportional to the vibration acceleration a_W of the windings, we then conclude that [15]

$$a_W \propto I^2. \quad (3)$$

Thus, similar to the case of core vibration, the fundamental frequency of winding vibrations is also twice the ac frequency. The difference between these two types of vibrations is that the magnitude of core vibration relies on the voltage applied to the primary windings and is not affected by the load current, while the magnitude of winding vibrations is proportional to the square of the loading current. In addition to the variables (voltage and current) causing transformer vibration, the other factors (i.e., temperature, power factor) also have an influence on vibration [13], but due to the relatively small influence, these factors are

not considered in this study. In fact, since power transformers in nuclear powerplants always operate at 100% full power, the variables (voltage and current) and the power factor generally exhibit very small variations over time. And since cooling systems can effectively keep transformers cores and windings at suitably low temperatures, the temperature factor also has very small fluctuation.

B. Vibration Signal Acquisition

In this study, 54 in-service power transformers in four nuclear powerplants were employed for acquiring vibration signals. Among these transformers, three are triple-phase transformers and the others are single-phase transformers. (See Table VIII.) These 54 transformers have a wide range of ages, from less than one year to about 22 years. This study employed B&K 4381 and PCB 357B33 accelerometers, which are charge types with charge amplifiers (RION UV-06A). Depending on the transformer size, 36 to 162 accelerometers were used to acquire the vibration signals from the transformers. The sensors were evenly positioned within 1 m on the single-phase and triple-phase main transformers, as respectively shown in Fig. 2(a) and (b). Measurements were conducted along two directions (X and Y) on the surface of the transformer frame and one perpendicular direction (Z) to the surface. The accelerometers were installed on the flat surface with a magnet base for easy measurement.

All measurements were obtained in the form of time-domain signals in a full-power operation state of the power transformers. In the state, all other subsidiary units affecting vibration under normal operating conditions, such as forced cooling systems and hydraulic pumps, were turned on. The subsidiary units were supplied with 480 V ac power. In most cases, the transformers

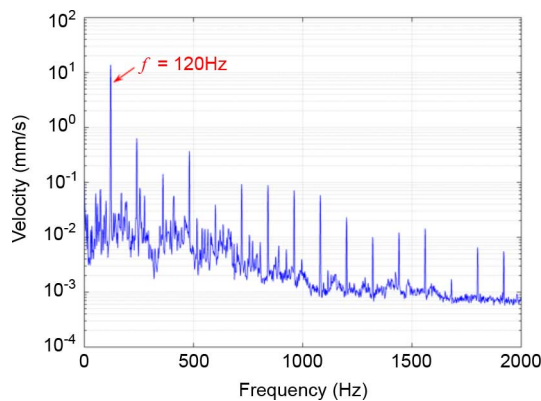


Fig. 3. Frequency spectral signal of a vibration velocity (YK).

convert primary electrical values (i.e., voltages 22 kV and currents about 32 kA) to proportional secondary values (i.e., voltages 345 kV and current about 2 kA). The measurement system was powered by an independent battery power system. Vibration velocity (in millimeters per second) was measured every 1.25 Hz in the frequency range of 0–2000 Hz. The rated voltage always has a frequency of 60 Hz. It is desirable to avoid taking the measurement immediately after turning the transformer on because the initial operation state of the transformer causes transient vibration signals. It is certainly important to acquire better sensory data and, thus, improve the performance of power transformer health diagnostics by optimizing the number of measure points and the allocation of the sensors. For the study regarding the sensor network optimization, readers are advised to look at [30].

C. Data Preprocessing

Given the fundamentals of the transformer vibration (see Section II-A), the use of the spectral response is strongly recommended for health metrics against the mechanical faults in the transformers. The vibration signals are thus processed using a fast Fourier transform (FFT). Fig. 3 displays a spectral response of a vibration signal, which has harmonic frequencies every 120 Hz. The amplitudes at these harmonic frequencies are significantly higher (more than ten times) than those at the other frequencies. As introduced in Section II-A, the fundamental frequencies of core and winding vibrations are twice the ac frequency (60 Hz), which is quite consistent with our observation in Fig. 3. Since the harmonic frequencies remain constant at every 120 Hz, the amplitudes at the harmonic frequencies could imply a degree of health state against the mechanical faults in the power transformers.

The spectral response amplitudes of the vibration velocities at 120 Hz were obtained from the 54 transformers. We computed the mean and maximum amplitudes of the vibration velocities measured by all sensors installed on each transformer and plotted these two quantities for all 54 transformers in Figs. 4 and 5, respectively. Two observations can be made from the two figures. First, both quantities exhibit large variations among different transformers. Specifically, the mean amplitudes of the vibration velocities have a wide range of variation from 1.43 to 18.87 mm/s and the maximum amplitudes from 5.8 to 136.43

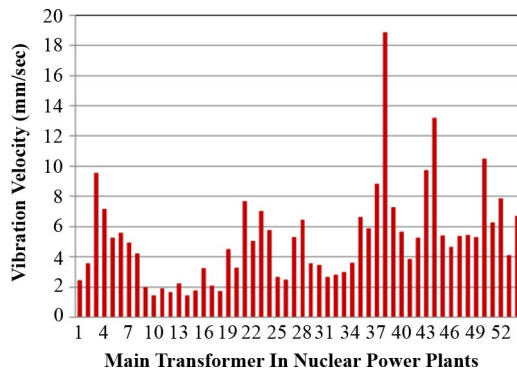


Fig. 4. Mean amplitudes of spectral responses at 120 Hz for 54 transformers.

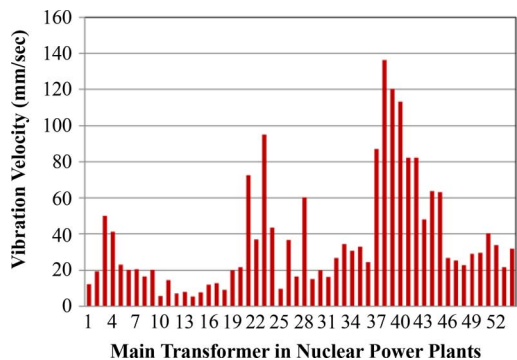


Fig. 5. Maximum amplitudes of spectral responses at 120 Hz for 54 transformers.

mm/s. It is believed that the aging effect of the transformers and local resonance of the transformer frame primarily cause the variation in the mean and maximum amplitudes. Second, the maximum velocity amplitude of each transformer is, in general, far greater than the mean velocity amplitude of that transformer. This observation can be attributed to the fact that among more than 40 measurement points selected for each transformer, two or three points at the upper part (closer to the top) of the transformer wall typically gave much larger velocities than the others.

III. HEALTH METRICS AND GRADE SYSTEM

This section presents the copula-based statistical health grade system against mechanical faults of power transformers.

A. Health Metrics

The frequency spectral signals from multiple sensors are employed to monitor the health condition of the power transformers. Two scalar health metrics are proposed in this study: 1) RMS and 2) RMS deviation (RMSD). Their definitions and physical meanings are given as follows.

- 1) **RMS**: The RMS is the quadratic measure of the vibration mean velocities measured at every 2.5 Hz in the frequency range of 2.5–2000 Hz. The RMS metric can be defined as

$$\text{RMS}_i = \left(\sum_{f=2.5 \text{ Hz}}^{2000 \text{ Hz}} \mu_f^2 \right)^{1/2}, \quad i = 1, \dots, 54 \quad (4)$$

where μ_f is the mean of the vibration velocity measured from all sensors at a frequency f . It is generally known that measured vibration velocities in the transformers become greater as their health state degrades over years. This metric is thus a useful health metric for transformer health monitoring. However, the magnitudes of the mean velocity also vary depending on the operating condition, the transformer capacity, and manufacturer. The RMS metric may fail to classify a health condition of different transformers experiencing mechanical degradation. This underscores the need for another health monitoring metric.

- 2) **RMSD**—The RMSD is the quadratic measure of the vibration deviation velocities measured at every 2.5 Hz in the frequency range of 2.5–2000 Hz. The RMSD metric can be defined as

$$\text{RMSD}_i = \left(\sum_{f=2.5 \text{ Hz}}^{2000 \text{ Hz}} \sigma_f^2 \right), i = 1, \dots, 54 \quad (5)$$

where σ_f is the standard deviation of the vibration velocity measured from all sensors at a frequency f . The same mean velocities could indicate different health conditions if the vibration measurements come from different transformers under random operating conditions. The undesirable situation discussed before can be avoided by using the RMS and RMSD since the randomness in operating conditions and the difference in transformers could affect the deviation of the vibration velocity.

In cases where we have mechanical defects (for example, winding deformations or loosened clamps in the core), the magnitudes of winding or core vibration typically increase because, as aged, electrodynamic forces (for winding) generally grow; mechanical constraints (for core) loosen, and structural strength becomes weaker. Moreover, the winding or core vibration typically becomes more stochastic and, to some degree, has variation over different transformer samples. For the very reason, the magnitude (mean) and randomness (standard deviation) of tank vibration amplitude increase. The RMS and RMSD measures are capable of capturing the transformer health degradation and its variation. For the power transformers we investigated (i.e., step-up transformers used in power plants), the mean and deviation of the vibration velocity at 120 Hz was generally observed to become higher as transformers get older.

The vibration signals measured from the fifty-four transformers in June 2006, February 2007, and August 2007 were processed to acquire a populated RMS and RMSD dataset as shown in Fig. 6. Since older transformers generally have larger RMS and RMSD values than newer ones, the two health metrics are highly correlated in a positive sense (see Fig. 6) with a Pearson’s linear correlation coefficient ρ being 0.9161. The transformers with a relatively good health condition are located at the lower left corner and the others at the upper right corner.

B. Copula-Based Statistical Health Grade System

As shown in Fig. 6, a strong statistical correlation exists between the proposed health metrics: RMS and RMSD. In what

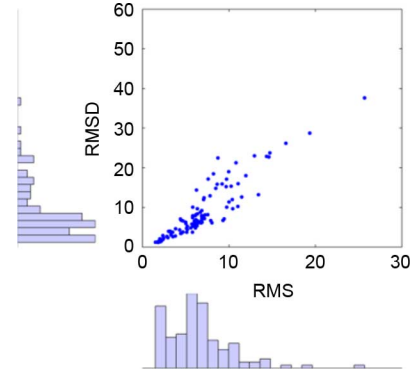


Fig. 6. Scatter plot and histograms of RMS and RMSD data (from 54 transformers in October 2006, February 2007, and August 2007).

follows, we intend to exploit this correlation using a joint statistical model—copulas. We start with a brief introduction on copulas. Next, we present three popular types of copulas. Finally, we detail the procedures to construct an appropriate copula for dependence modeling based on available data.

1) *Introduction of Copulas*: In statistics, a copula is defined by Roser [26] as “a function that joins or couples multivariate joint distribution functions to their 1-D marginal distribution functions”, or “multivariate distribution functions whose 1-D margins are uniform on the interval $[0, 1]$.” In other words, a copula formulates a joint cumulative distribution function (CDF) based on marginal CDFs and a dependence structure. In the following description, we will see that copulas allow one to decouple the univariate marginal distribution modeling from multivariate dependence modeling.

Let $\mathbf{x} = (x_1, x_2, \dots, x_N)$ be an N -dimensional random vector with real-valued random variables, and F be an N -dimensional CDF of \mathbf{x} with continuous marginal CDFs F_1, F_2, \dots, F_N . Then, according to Sklar’s theorem, a unique N -copula C exists such that

$$F(x_1, x_2, \dots, x_N) = C(F_1(x_1), F_2(x_2), \dots, F_N(x_N)). \quad (6)$$

It then becomes clear that a copula formulates a joint CDF with the support of separate marginal CDFs and a dependence structure. This decoupling between marginal distribution modeling and dependence modeling is an attractive property of copulas, since it leads to the possibility of building a wide variety of multivariate densities. In real applications, this possibility can be enabled by employing different types of marginal CDFs or dependence structures. Based on (6) and under the assumption of differentiability, we can derive the joint probability density function (PDF) of the random vector \mathbf{x} , expressed as

$$\begin{aligned} f(x_1, x_2, \dots, x_N) \\ = c(F_1(x_1), F_2(x_2), \dots, F_N(x_N)) \cdot \prod_{i=1}^N f(x_i) \end{aligned} \quad (7)$$

where c is the joint PDF of the copula C . Equation (7) suggests that a joint PDF of \mathbf{x} can be constructed as the product of its marginal PDFs and a copula PDF. The PDF formulation in (7) is useful in formulating a likelihood function and estimating the parameters of marginal PDFs and a copula, as will be discussed later.

2) *Copula Types*: Various general types of dependence structures can be represented, corresponding to various copula families. In what follows, we will briefly introduce four popular copula types, that is, Gaussian, Clayton, Frank, and Gumbel. More detailed information on copula families can be found in [26].

Let $u_i = F_i(x_i)$ and $i = 1, 2, \dots, N$, an N -dimensional Gaussian copula with a linear correlation matrix Σ is defined as

$$C_G(u_1, u_2, \dots, u_N | \Sigma) = \Phi_N \left(\begin{array}{c} \Phi^{-1}(u_1), \Phi^{-1}(u_2), \\ \dots, \Phi^{-1}(u_N) \end{array} | \Sigma \right). \quad (8)$$

where Φ denotes the joint CDF of an N -dimensional standard normal distribution and Φ^{-1} denotes the inverse CDF of a 1-D standard normal distribution. It is noted that Σ is a symmetric matrix with diagonal elements ρ_{ii} being ones, for $i = 1, 2, \dots, N$, and offdiagonal elements ρ_{ij} being the pairwise correlations between the pseudo Gaussian random variables $z_i = \Phi^{-1}(u_i)$ and $z_j = \Phi^{-1}(u_j)$, for $i, j = 1, 2, \dots, N$ and $i \neq j$.

Another popular copula family is an N -dimensional Archimedean copula, defined as

$$C_A(u_1, u_2, \dots, u_N | \alpha) = \Psi_\alpha^{-1} \left(\sum_{i=1}^N \Psi_\alpha(u_i) \right) \quad (9)$$

where Ψ_α denotes a generator function with a correlation parameter α and satisfies the following conditions:

$$\begin{aligned} \Psi_\alpha(1) &= 0; \lim_{u \rightarrow 0} \Psi_\alpha(u) = \infty; \\ \frac{d}{du} \Psi_\alpha(u) &< 0; \frac{d^2}{du^2} \Psi_\alpha(u) > 0. \end{aligned} \quad (10)$$

Commonly used Archimedean copulas are Clayton, Frank, and Gumbel copulas, which are summarized in Table II. To exemplify the diversity of copulas, we present the scatter plots of the aforementioned four copulas with Kendall's tau (τ) coefficients being 0.70 in Fig. 7, where we can observe significant difference in dependence patterns modeled by different copulas.

3) *Fitting Copula Model*: In this section, we aim to determine the most appropriate copula model C with marginal CDFs F to model the dependence of a random vector \mathbf{x} . Suppose that we have M independent random samples from a multivariate distribution, $\{\mathbf{x}_j = (x_{1j}, x_{2j}, \dots, x_{Nj}), j = 1, 2, \dots, M\}$. Let β be the vector of marginal distributional parameters and α be the vector of copula parameters. The procedure to fit a copula model is detailed as the following three steps:

Step 1) (*Parameter Estimation*): The aim of this step is to estimate the parameters β and α . This can be done with the maximum-likelihood method (MLE). According to (7), the log-likelihood function to be maximized is

$$\begin{aligned} f(x_1, x_2, \dots, x_N) &= \sum_{j=1}^M \log c \left(\begin{array}{c} F_1(x_{1j}; \beta), F_2(x_{2j}; \beta), \dots, \\ F_N(x_{Nj}; \beta); \alpha \end{array} \right) \\ &\quad + \sum_{i=1}^N \sum_{i=1}^M \log f_i(x_{ij}; \beta). \end{aligned} \quad (11)$$

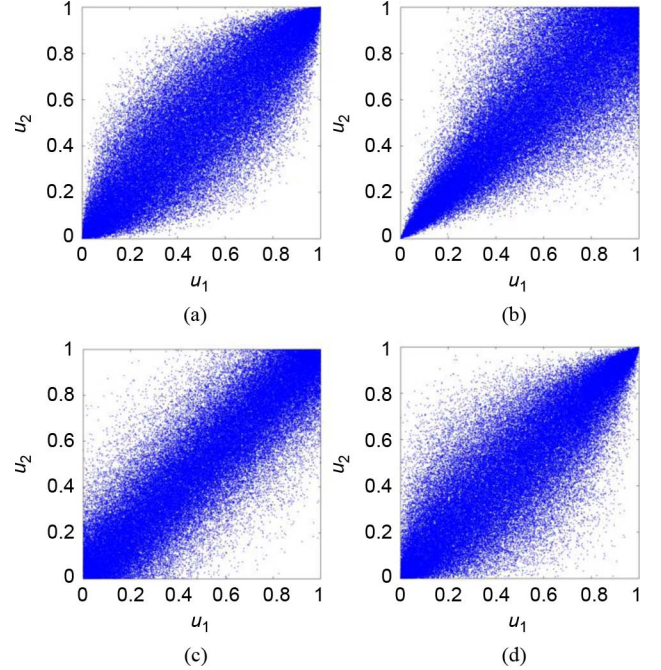


Fig. 7. Scatter plots of various copulas with Kendall's tau (τ) coefficients being 0.70: (a) Gaussian, (b) Clayton, (c) Frank, and (d) Gumbel.

TABLE II
SUMMARY OF THREE ARCHIMEDEAN COPULAS.

Family	Generator $\Psi_\alpha(u)$	Bivariate copula $C_A(u_1, u_2 \alpha)$	Parameter space
Clayton	$u^{-\alpha} - 1$	$(u_1^{-\alpha} + u_2^{-\alpha} - 1)^{-1/\alpha}$	$\alpha > 0$
Frank	$-\ln \frac{e^{-\alpha u} - 1}{e^{-\alpha} - 1}$	$-\frac{1}{\alpha} \left\{ 1 + \frac{[(e^{-\alpha u_1} - 1)][e^{-\alpha u_2} - 1]}{e^{-\alpha} - 1} \right\}^{-1/\alpha}$	$\alpha > 0$
Gumbel	$(-\ln u)^\alpha$	$\exp \left\{ - \left[(-\ln u_1)^\alpha + (-\ln u_2)^\alpha \right]^{1/\alpha} \right\}$	$\alpha > 0$

Since we generally do not have closed-form solutions to globally maximize the above likelihood function, the simultaneous estimation of the marginal distributional and copula parameters is computationally expensive. To alleviate the computational burden, we employ a two-stage estimation method called the inference functions for margins (IFM) method, proposed by Joe [27]. The IFM method decomposes the estimation of the parameters β and α into two steps. In the first step, it estimates the marginal distributional parameters β by maximizing the second log-likelihood term in (11). With the estimated parameters β and, thus, known marginal distributions, the second step then estimates the copular parameters α by maximizing the first log-likelihood term in (11).

Step 2) (*Goodness-of-Fit Test*): In this step, we intend to test whether a specific copula model with estimated parameters from Step 1 fits the samples with sufficient

accuracy. For this purpose, we propose to employ the Kolmogorov–Smirnov (K-S) distance [28], expressed as

$$D_{KS} = \int |F_e - F_n| dF_n \quad (12)$$

where F_e denotes the empirical CDF derived from the random samples, and F_n denotes the hypothesized CDF. We note that to reduce the influence of outliers on the K-S distance and reflect the overall fitting quality, we computed an average absolute difference instead of a maximum one. When we test the fit of a specific marginal distribution, both F_e and F_n are univariate CDFs with the inputs being random variables $x_i, i = 1, 2, \dots, N$. In contrast, when we test the fit of a specific copula, F_e and F_n , respectively, become an empirical joint CDF and a hypothesized copula both of which take vectors of marginal probabilities \mathbf{u} as inputs.

Step 3) (*Goodness-of-Fit Retest*): To decide whether the distance measure in (12) provides sufficient evidence on the good fit of the copula, we retest the good of fit of the copula model by generating random samples of the size M under the assumption that the null hypothesis of an accurate fit is true [29]. We repeatedly execute the retesting process K times to generate K sets of random samples and, correspondingly, obtain K distance measures by executing the aforementioned Steps 1) and 2). For each retest, we generate random samples with two steps: 1) generate sample pairs (u_{1j}, u_{2j}) of $[0, 1]$ uniform distributed random variables u_{1j} and u_{2j} according to the copula model with the parameters α estimated in Step 1, and 2) transform the sample pairs (u_{1j}, u_{2j}) to observation pairs (x_{1j}, x_{2j}) with the inverse marginal CDFs F_1^{-1} and F_2^{-1} . Finally, we construct a probability distribution of the distance measure D_{KS} and determine the p -value, or the probability of observing a distance measure at least as extreme as the value obtained in Step 2) under the assumption of an accurate copula fit.

4) *Building a Copula-Based Statistical Health Grade System*: In this section, we apply the aforementioned copula model to representing the joint distribution of the RMS and RMSD metrics by modeling the dependence between these two. Upon construction of the joint distribution, we then define a statistical health grade system based on the joint CDF of the two health metrics.

Data Statistics and Marginal Distributions: Table III presents summary statistics on the populated RMS and RMSD data as well as the types and parameters of fitted marginal distributions. Compared to the RMS, the RMSD yields a larger mean value and a much larger variance. Kurtosis values are very high for both metrics, indicating that a large portion of the variance is contributed to by infrequent extreme deviations. This can also be observed from the histograms of the two metrics in Fig. 8, where we observe a considerable amount of extreme data for any of the two metrics. Results from the K-S

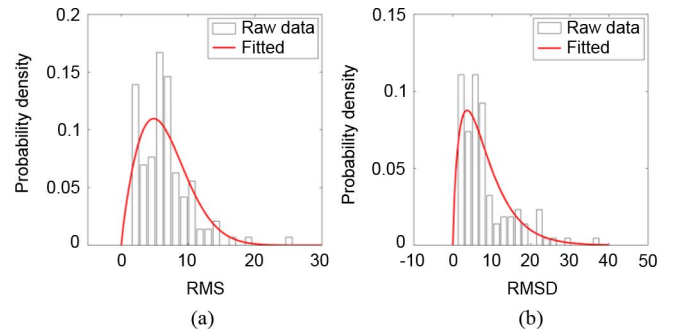


Fig. 8. Histograms and fitted distributions of (a) RMS and (b) RMSD.

TABLE III
SUMMARY OF DATA STATISTICS AND FITTED MARGINAL DISTRIBUTIONS

Health metric	Data statistics					
	Mean	Std ^a	Skewness	Kurtosis	Minimum	Maximum
RMS	6.57	3.81	1.66	7.99	1.51	25.68
RMSD	8.27	6.64	1.64	6.04	1.20	37.63
Health metric	Fitted marginal distribution					
	Type	Parameters ^b				
RMS	Weibull	$\beta_1 = 7.42, \beta_2 = 1.84$				
RMSD	Gamma	$\beta_3 = 1.78, \beta_4 = 4.64$				

^a Standard deviation

^b Scale and shape parameters for Weibull and gamma distributions

test suggest that the RMS and RMSD data be statistically modeled with the Weibull and gamma distributions, respectively. The parameters of the fitted marginal distributions are given in Table III, and their plots are presented in Fig. 8.

Copula Model: We used the aforementioned procedure to identify an appropriate copula model from the four candidates, that is, Gaussian, Clayton, Frank, and Gumbel copulas. Table IV summarizes the copula fitting results based on the populated RMS and RMSD data. Both the correlation estimate in Gaussian copula and α estimates in three Archimedean copulas indicate a strong correlation between the RMS and RMSD. Regarding the retest, we generated 10 000 sets (i.e., $K = 10\,000$) of random samples under the null hypothesis of an accurate copula fit and ran each of the 10 000 sets through the aforementioned Steps 1 (Parameter Estimation) and 2 (Goodness-of-Fit Test) to obtain 10 000 distance measures. It can be observed that any of the four copulas cannot be rejected under the commonly used significance level 0.05. This can be partially attributed to the fact that we only have a relatively small number of data. We conjecture that as we have more data, the p -values yielded by different copulas will become more distinctive and an appropriate copula model can be selected with more confidence. Out of the four copulas, Gaussian copula produced the smallest distance measure D_{KS} and the largest p -value, which offers us supporting evidence of the best fit provided by Gaussian copula. The histogram of D_{KS} of Gaussian copula is plotted with the estimated D_{KS} in Fig. 9(a). To verify the accuracy of fit, we synthetically generated 1000 random samples from the fitted Gaussian

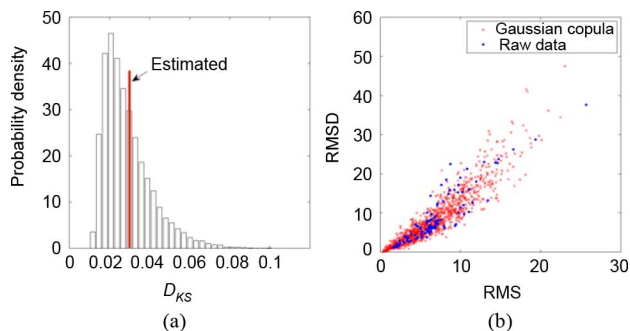


Fig. 9. Histograms of (a) DKS and (b) scatter plot of the Gaussian copula.

TABLE IV
COPULA FITTING RESULTS

Copula type	Parameter estimation ^a			Test and retest	
	Point estimate	Standard error	95% confidence interval ^b	D_{KS} estimate	p -value ^c
Gaussian	0.930	0.012	(0.906, 0.955)	0.0300	0.3684
Clayton	6.035	0.688	(4.685, 7.385)	0.0330	0.3216
Frank	15.095	1.384	(12.382, 17.809)	0.0324	0.2916
Gumbel	3.484	0.194	(3.103, 3.864)	0.0326	0.2642

^a Linear correlation coefficient for Gaussian, α in Table II for the rest

^b Point estimate ± 1.96 -standard error

^c With 10,000 simulations

copula model and plot these samples together with the raw data in Fig. 9(b). We can observe a generally accuracy representation of the raw data, especially in the lower-left region. The synthetic samples were generated by following the same steps we used to generate the 10 000 random sets for the retest: first drawing uniform samples from the copula and then transforming these samples back to the original Weibull and gamma samples using the inverse CDFs of these distributions.

Health Grade System: We quantify the health condition for a specific transformer unit (i.e., a specific RMS and RMSD pair) by the proportion of the population with larger RMS and RMSD values than that unit. Let x_1 and x_2 denote the health metrics RMS and RMSD, respectively. Let $C(F_1(x_1), F_2(x_2))$ denote the copula model we derived from the previous section with $F_1(x_1)$ and $F_2(x_2)$ being the marginal CDFs of x_1 and x_2 . Mathematically, the health condition h of a health metric pair (x_{1d}, x_{2d}) can be defined in terms of marginal CDFs and a joint CDF or copula, expressed as

$$h(x_{1d}, x_{2d}) = \Pr(x_1 > x_{1d}, x_2 > x_{2d}). \quad (13)$$

This can be further derived as a function of the marginal CDFs of x_1 and x_2 and the copula, expressed as

$$\begin{aligned} h(x_{1d}, x_{2d}) &= \Pr(u_1 > F_1(x_{1d}), u_2 > F_2(x_{2d})) \\ &= \Pr(u_1 > F_1(x_{1d}) - \Pr(u_2 \leq F_2(x_{2d})) \\ &\quad + \Pr(u_1 \leq F_1(x_{1d}), u_2 \leq F_2(x_{2d})) \\ &= 1 - F_1(x_{1d}) - F_2(x_{2d}) \\ &\quad + C(F_1(x_{1d}), F_2(x_{2d})). \end{aligned} \quad (14)$$

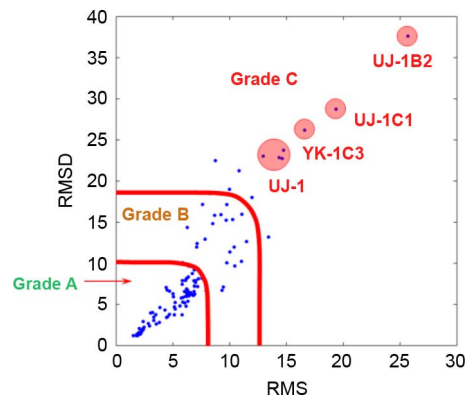


Fig. 10. Statistical health grade map.

It is noted that, in the above equation, we define the health condition of a transformer unit as the probability of a joint event rather than a union one. The aim of this definition is to achieve a certain level of conservativeness since the mechanical failure of a power transformer causes significant monetary and societal losses and is rather undesirable.

Based on the health condition defined in (14), we further defined three health grades which, from the perspective of probability, can be mapped to three ranges in a zero-mean normal distribution, that is, below 1.0σ , between 1.0σ and 2.0σ and above 2.0σ , as shown in Table V. Table VI relates the three health grades to suggested maintenance actions. Experts' experience and historic information on inspection and maintenance of the power transformers over the years were employed to derive the relationship. Fig. 10 visualizes the three health grades in the RMS-RMSD map, where the boundaries were identified by equating the health condition in (14) to the two critical health conditions in Table V and deriving the corresponding joint probability contours. The transformers that are classified into Grade A turned out to be relatively newer transformers (average life about 6 years old), whereas those with Grades B and C were relatively older transformers (average life about 30 years old). To verify the feasibility of the proposed health grade system, we looked at the oldest transformers (UJ1, YK1) more closely. The health grades of the transformers were identified with "Grade C" which indicates that inspection and maintenance actions must be executed immediately. It has been confirmed by the experts that the transformers' health conditions were critical and they were recently replaced with new transformers. This indicates that the proposed grade system properly defines the health condition of the transformers against mechanical faults. Finally, we note that the boundaries (1.0σ and 2.0σ standard normal lines) adopted in this paper might not be directly applicable for all practical use cases and certain customizations need to be made to satisfy a particular need. It is noted, however, that the procedure to build a statistical health grade system is general in the sense that it is directly applicable to all use cases. Moreover, field experts will make a final decision on maintenance while using this classification as a reference.

TABLE V
DEFINITION OF THREE HEALTH GRADES.

Health Grade	A	B	C
Health condition	$h > 0.16$	$0.02 < h \leq 0.16$	$h \leq 0.02$
σ -level of standard normal distribution	$z < 1.0\sigma$	$1.0\sigma \leq z < 2.0\sigma$	$z \geq 2.0\sigma$

TABLE VI
MAINTENANCE ACTIONS ON HEALTH GRADES.

Health Grade	Health Conditions and Suggested Maintenance Actions
Grade A (Healthy)	Excellent health condition – Health condition is excellent; transformer requires least frequent inspection and maintenance.
Grade B (Warning)	Transitional health condition – Health condition has partial degradation; transformer requires more frequent inspection (e.g., in-situ monitoring) to obtain health metric data that can be related to health condition; condition-based maintenance (CBM) should be considered on the basis of remaining useful life (RUL) prediction by health prognostics.
Grade C (Faulty)	Critical health condition – Health condition is close to failure due to mechanical faults in a component level; field engineers need to identify fault type, location, and severity; transformer requires an immediate replacement of faulty mechanical components to avoid entire transformer failure if they can be identified.

C. Feasibility Study of Health Prognostics

Prognostics is the discipline of predicting the RULs of engineered systems over the lifetime. To make the life prognostics useful, a significant amount of health condition (RMS and RMSD) data must be acquired from a set of homogeneous transformers. Given the limited available data sets obtained in June 2006, February 2007, and August 2008, this study is intended not to develop a rigorous life prognostics model but to conduct a feasibility study for the life prognostics. This feasibility study was performed with the data sets from the power transformers in the WS nuclear powerplant. The copula model transformed the 2-D health metrics (RMS and RMSD) into the 1-D health condition using (14), which was then used for observing and predicting the health degradation in the lifetime of the transformers. The RMS and RMSD data from the transformers in the WS plant were plotted and sorted by the measured time, as shown in Fig. 11(a). Note that the vibration measurements were taken from all 54 transformers in June 2006, February 2007, and August 2007, providing a total of 3×54 data samples. The health degradation of transformer core joints is demonstrated over time in Fig. 11, where six same-type (or homogeneous) transformers out of 54 are used and indeed shows a clear degradation trend. The variation in two health metrics is mainly due to different capacities of the transformers and randomness in the operation conditions. As time passed from June 2006 to August 2007, the health condition metrics became higher. This indicates that the health condition degradation can be distinctively observed by monitoring the health condition metrics. Generally, the linear, exponential, power, and logarithmic models are basic mathematical models that can be used to extrapolate the degradation

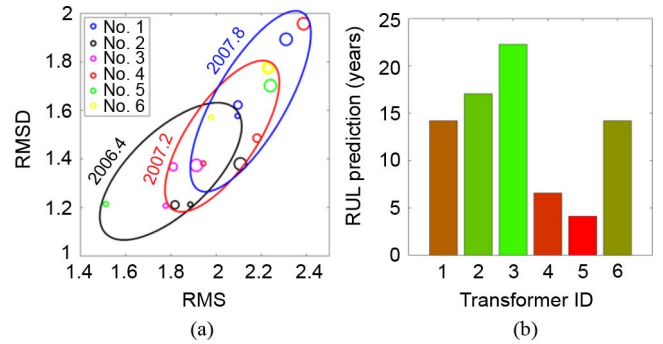


Fig. 11. (a) Health degradation history and (b) predicted RULs for power transformers (WS).

TABLE VII
SPECIFICATIONS OF ALL TRANSFORMERS IN KORI, YK, UJ, AND WS

Location	Unit	Type	Manufacture	Voltage (High/Low, kV)	Capacity (MVA, at 55°C)
KORI	1	3 phase	hyosung	362/22	750
	2	3 phase	hyosung	362/22	790
	3	1 phase	hyosung	362/22	385 * 3
	4	1 phase	hyosung	362/22	385 * 3
YK	1	1 phase	hyosung	362/22	403 * 3
	2	1 phase	hyosung	362/22	403 * 3
	3	1 phase	hyosung	345/20.9	353.3 * 3
	4	1 phase	hyosung	345/20.9	353.3 * 3
	5	1 phase	hyosung	345/20.9	353.3 * 3
	6	1 phase	hyosung	345/20.9	353.3 * 3
WS	1	3 phase	Hyundai	362/26	840
	2	1 phase	Hyundai	345/22	277 * 3
	3	1 phase	Hyundai	345/22	277 * 3
	4	1 phase	Hyundai	345/22	277 * 3
UJ	1	1 phase	hyosung	362/22	372.8 * 3
	2	1 phase	hyosung	362/22	372.8 * 4
	3	1 phase	hyosung	345/20.9	353.3 * 3
	4	1 phase	hyosung	345/20.9	353.3 * 3
	5	1 phase	hyosung	345/20.9	353.3 * 3
	6	1 phase	hyosung	345/20.9	353.3 * 3

measurements to the defined failure level in order to estimate the failure time. As shown in Fig. 10, the health degradation behaves exponentially, increasing slowly at the early life of the transformer but rapidly at the end of the life. Thus, we used the exponential model to capture the transition trend of the health condition and extrapolated the exponential model to a failure threshold ($h = 0$) to obtain the remaining useful life. The health prognostics results for the six transformer units are graphically shown in Fig. 11(b), where the predicted RULs range from less than 5 years to above 20 years.

IV. CONCLUSION

This paper presented a copula-based statistical health grade system against mechanical faults of power transformers in nuclear powerplants. The vibration signal signatures acquired from the power transformers were used to define two health metrics (RMS and RMSD). The populated metrics data from 54 power transformers were used to identify an appropriate copula model, based on which a statistical health grade system is built with corresponding health conditions and suggested maintenance actions. The copula-based statistical health grade system can be useful for making maintenance decisions, while

TABLE VIII
RMS AND RMSD FOR ALL TRANSFORMERS IN YK, UJ, AND WS

Location	Unit	Phase	04/2006		02/2007		08/2007	
			RMS	RMSD	RMS	RMSD	RMS	RMSD
YK	1	A						
		B			3.4935	3.7586	4.4083	4.7433
		C	10.8184	21.2638	9.6774	15.2434	11.9149	18.7117
	2	A	6.1644	8.0906	5.8147	7.4488	7.2082	9.1807
		B	8.2268	18.4866	6.2618	14.3723	7.7437	17.7022
		C	7.0891	11.9838	5.8223	7.8991	7.2067	9.7351
	3	A	3.5302	2.6278	2.9425	2.3837	3.7121	3.0416
		B	8.7348	22.4859	4.4078	7.0695	5.4724	8.7757
		C	6.2146	8.1801	5.7957	3.7542	7.4235	4.8832
	4	A	7.0048	7.9036	6.3626	9.68	8.0392	12.0284
		B	5.8535	5.2815	4.4444	3.4313	5.5571	4.295
		C	4.5239	3.5049	3.3184	3.4511	4.1653	4.2948
	5	A	8.0345	6.1175	3.3179	3.0496	4.2151	3.8115
		B	6.4082	6.0413	3.8493	4.6327	4.8549	5.7959
		C	10.2612	15.3348	4.6928	6.6165	5.7945	8.1362
	6	A	6.2767	6.7398	5.002	6.2901	6.1577	7.7343
		B	6.3487	8.3477	6.9783	7.6711	8.5739	9.4235
		C	6.3093	6.2303	6.2191	6.3663	7.6363	7.8104
UJ	1	A						
		B			25.683	37.6344		
		C	19.3516	28.7425	14.738	23.756	8.4941	14.8265
	2	A	9.9755	19.0113	12.9438	23.0255	14.619	22.7439
		B	11.0612	15.9743	8.6555	15.8371	11.9566	18.0058
		C	14.3538	22.8637	9.2198	15.9236	7.2417	8.1277
	3	A	6.1895	5.9806	10.0143	11.3763	6.5462	6.4366
		B	11.4765	12.6484	13.4102	13.199	9.7375	10.0747
		C	9.7347	17.1477	6.8758	9.2086	6.8016	6.0879
	4	A	7.1267	12.411	6.1393	6.0104	7.8248	12.9405
		B	4.6828	3.7881	6.0354	5.198	6.9082	6.2445
		C	3.0354	3.976	6.1473	4.7841	6.8478	7.8904
	5	A	6.8923	7.2407	5.1924	5.2341	6.7011	8.7737
		B	11.0317	10.2376	9.4405	7.1195	10.4389	9.6835
		C	5.7305	5.792	6.0117	6.5637	5.8994	5.8661
	6	A	6.195	6.8874	7.1765	7.1809	7.5634	8.1893
		B	6.1051	7.9166	5.114	4.7147	5.8188	10.0799
		C	6.4567	6.1449	6.3587	6.4674	6.8919	7.2125
WS	1	A						
		B					2.2402	1.702
		C	1.5119	1.2139			2.8317	2.6835
	2	A	1.5119	1.2139				
		B			2.1804	1.4858	2.3866	1.9573
		C	1.9431	1.3812				
	3	A	2.0948	1.5776	2.0962	1.6223	2.3091	1.8932
		B	1.8853	1.2124	1.8178	1.2107	2.1066	1.3798
		C	1.7767	1.207	1.8101	1.3677	1.9125	1.3735
	4	A	2.3797	2.9213	2.3555	2.0227	2.3555	2.0227
		B	2.0295	2.0761	2.4585	2.2441	2.4585	2.2441
		C	1.9772	1.5718	2.2301	1.7756	2.2301	1.7756

monitoring the health conditions of the power transformers. It is noted that uncertainties in manufacturing conditions, operation conditions, and measurements further propagate to uncertainties in the two health metrics. Thus, a health grade system should not only be characterized by its diagnostic accuracy but also by its ability to perform the diagnostics in a statistical manner. In this light, the proposed statistical health grade system offer researchers and industrial practitioners a powerful tool to systematically capture the aforementioned uncertainties and build statistical power in defining health grades. To investigate the feasibility of the proposed statistical health grade system for health prognostics, we established an exponential model to capture the transition trend of the health condition and predicted the remaining useful life by extrapolation. Finally, we conclude that the copula model is capable of characterizing the statistical dependence between the two health metrics, and that

the health condition defined based on this model is an attractive health measure suitable for health prognostics.

REFERENCES

- [1] W. R. Lee, S. W. Jung, K. H. Yang, and J. S. Lee, "A study on the determination of subjective vibration velocity ratings of main transformers under operation in nuclear power plants," presented at the 12th Int. Congr. Sound Vibr., Lisbon, Portugal, Jul. 11–14, 2005.
- [2] M. Wang, A. J. Vandermaar, and K. D. Srivastava, "Review of condition assessment of power transformers in service," *IEEE Elect. Insul. Mag.*, vol. 18, no. 6, pp. 12–25, Nov./Dec. 2002.
- [3] M. K. Pradhan, "Assessment of the status of insulation during thermal stress accelerated experiments on transformer prototypes," *IEEE Trans. Dielect. Elect. Insul.*, vol. 13, no. 1, pp. 227–237, Feb. 2006.
- [4] T. K. Saha, "Review of modern diagnostic techniques for assessing insulation condition in aged transformers," *IEEE Trans. Dielect. Elect. Insul.*, vol. 10, no. 5, pp. 903–917, Oct. 2003.
- [5] S. D. J. McArthur, S. M. Strachan, and G. Jahn, "The design of a multi-agent transformer condition monitoring system," *IEEE Trans. Power Del.*, vol. 19, no. 4, pp. 1845–1852, Oct. 2004.
- [6] *IEEE Guide for the Interpretation of Gases Generated in Oil-Immersed Transformers*, IEEE Standard C57.104, 2008.
- [7] E. P. Dick and C. C. Erven, "Transformer diagnostic testing by frequency response analysis," *IEEE Trans. Power App. Syst.*, vol. PAS-97, no. 6, pp. 2144–2153, Nov. 1978.
- [8] B. Garcia, J. C. Burgos, A. M. Alonso, and J. Sanz, "A moisture-in-Oil model for power transformer monitoring-part II: Experimental verification," *IEEE Trans. Power Del.*, vol. 20, no. 2, pt. 2, pp. 1423–1429, Apr. 2005.
- [9] W. H. Tang, Q. H. Wu, and Z. J. Richardson, "A simplified transformer thermal model based on thermal-electric analogy," *IEEE Trans. Power Del.*, vol. 19, no. 3, pp. 1112–1119, Jul. 2004.
- [10] A. F. Picanço, M. L. B. Martinez, and C. R. Paulo, "Bragg system for temperature monitoring in distribution transformers," *Elect. Power Syst. Res.*, vol. 80, no. 1, pp. 77–83, 2010.
- [11] N. A. Muhamad and S. A. M. Ali, "Simulation panel for condition monitoring of oil and dry transformer using labVIEW with fuzzy logic controller," *J. Eng., Comput. Technol.*, vol. 14, pp. 187–193, 2006.
- [12] L. Gong, C.-H. Liu, and X. F. Zha, "Model-based real-time dynamic power factor measurement in AC resistance spot welding with an embedded ANN," *IEEE Trans. Ind. Electron.*, vol. 54, no. 3, pp. 1442–1448, Jun. 2007.
- [13] C. Bartoletti, M. Desiderio, D. Di Carlo, G. Fazio, F. Muzi, G. Sacerdoti, and F. Salvatori, "Vibro-acoustic techniques to diagnose power transformers," *IEEE Trans. Power Del.*, vol. 19, no. 1, pp. 221–229, Apr. 2004.
- [14] S. Ji, Y. Luo, and Y. Li, "Research on extraction technique of transformer core fundamental frequency vibration based on OLCM," *IEEE Trans. Power Del.*, vol. 21, no. 4, pp. 1981–1988, Oct. 2006.
- [15] B. Garcia, J. C. Burgos, and A. M. Alonso, "Transformer tank vibration modeling as a method of detecting winding deformations-part I: theoretical foundation," *IEEE Trans. Power Del.*, vol. 21, no. 1, pp. 157–163, Jan. 2006.
- [16] B. Garcia, J. C. Burgos, and A. M. Alonso, "Transformer tank vibration modeling as a method of detecting winding deformations-part II: Experimental verification," *IEEE Trans. Power Del.*, vol. 21, no. 1, pp. 164–169, Jan. 2006.
- [17] Y. C. Huang, "Evolving neural nets for fault diagnosis of power transformers," *IEEE Trans. Power Del.*, vol. 18, no. 3, pp. 843–848, Jul. 2003.
- [18] X. Hao and S. Cai-xin, "Artificial immune network classification algorithm for fault diagnosis of power transformer," *IEEE Trans. Power Del.*, vol. 22, no. 2, pp. 930–935, Apr. 2007.
- [19] Y. Hong-Tzer and L. Chiung-Chou, "Adaptive fuzzy diagnosis system for dissolved gas analysis of power transformers," *IEEE Trans. Power Del.*, vol. 14, no. 4, pp. 1342–1350, Oct. 1999.
- [20] Q. Su, C. Mi, L. L. Lai, and P. Austin, "A fuzzy dissolved gas analysis method for the diagnosis of multiple incipient faults in a transformer," *IEEE Trans. Power Syst.*, vol. 15, no. 2, pp. 593–598, May 2000.
- [21] P. Purkait and S. Chakravorti, "Time and frequency domain analyzes based expert system for impulse fault diagnosis in transformers," *IEEE Trans. Dielect. Elect. Insul.*, vol. 9, no. 3, pp. 433–445, Jun. 2002.
- [22] T. K. Saha and P. Purkait, "Investigation of an expert system for the condition assessment of transformer insulation based on dielectric response measurements," *IEEE Trans. Power Del.*, vol. 19, no. 3, pp. 1127–1134, Jul. 2004.

- [23] S.-W. Fei, C.-L. Liu, and Y.-B. Miao, "Support vector machine with genetic algorithm for forecasting of key-gas ratios in oil-immersed transformer," *Expert Syst. Appl.*, vol. 36, no. 3, pp. 6326–6331, 2009.
- [24] S. Fei and X. Zhang, "Fault diagnosis of power transformer based on support vector machine with genetic algorithm," *Expert Syst. Appl.*, vol. 36, no. 8, pp. 11352–11357, 2009.
- [25] H. J. Shin and S. Cho, "Response modeling with support vector machines," *Expert Syst. Appl.*, vol. 30, no. 4, pp. 746–760, 2006.
- [26] B. N. Roser, *An Introduction to Copulas*. New York: Springer, 1999.
- [27] H. Joe, *Multivariate Models and Dependence Concepts*. In: *Monographs on Statistics and Applied Probability*. London, UK: Chapman & Hall, 1997, vol. 73.
- [28] M. Chakravarti, R. G. Laha, and J. Roy, *Handbook of Methods of Applied Statistics*. New York: Wiley, 1967, vol. I, pp. 392–394.
- [29] E. Kole, K. Koedijk, and M. Verbeek, "Selecting copulas for risk management," *J. Banking Finance*, vol. 31, no. 8, pp. 2405–2423, 2007.
- [30] P. Wang, B. D. Youn, and C. Hu, "A generic sensor network design framework based on a detectability measure," presented at the ASME Int. Design Eng. Tech. Conf. Comput. Inf. Eng. Conf., Montreal, QC, Canada, Aug. 18, 2010.



Chao Hu received the B.E. degree in engineering physics from Tsinghua University, Beijing, China, in 2003, and the Ph.D. degree in mechanical engineering from the University of Maryland, College Park, in 2011.

Currently, he is a Senior Reliability Engineer with Medtronic, Inc., Minneapolis, MN. His research work has led to more than 30 journal and conference publications in the below areas. His research interests are system reliability analysis, prognostics and health management, and battery power and health

management of the lithium-ion battery system.



Pingfeng Wang received the B.E. degree in mechanical engineering from The University of Science and Technology, Beijing, China, in 2001, the M.S. degree in applied mathematics from Tsinghua University, Beijing, China, in 2006, and the Ph.D. degree in mechanical engineering from the University of Maryland, College Park.

Currently, he is an Assistant Professor in the Department of Industrial and Manufacturing Engineering, Wichita State University, Wichita, KS. His research interests are system reliability analysis,

risk-based design, and prognostics and health management.



Byeng D. Youn received the Ph.D. degree in mechanical engineering from the University of Iowa, Iowa City, IA, in 2001.

He was a Research Associate with the University of Iowa until 2004, an Assistant Professor with Michigan Technological University, Houghton, MI, until 2007, and an Assistant Professor with the University of Maryland, College Park, until 2010. Currently, he is an Associate Professor with the School of Mechanical and Aerospace Engineering, Seoul National University, Seoul, Korea. His research is dedicated to well-balanced experimental and simulation studies of

system analysis and design, and he is currently exploring three research avenues: system risk-based design, prognostics and health management (PHM), and energy harvester design.

Dr. Youn's research and educational dedication has led to: six notable awards, including the ISSMO/Springer Prize for the Best Young Scientist in 2005 from the International Society of Structural and Multidisciplinary Optimization (ISSMO), and more than 100 publications in the area of system-risk-based design and PHM and energy harvester design.



Wook-Ryun Lee received the B.Sc. degree in mechanical engineering from Yonsei University, Seoul, Korea, in 1997 and the M.Sc. degree in mechanical engineering from Chungnam National University, Chungnam, Korea, in 2004.

Currently, he is a Senior Researcher with the Green Energy Laboratory, Research Institute, Korea Electric Power Corporation, Daejeon, Korea. His research interests are control of noise and vibration generated from powerplants, and kinetic energy storage systems, such as flywheel energy storage,

energy harvesting, etc.



Joung Taek Yoon received the B.S. degree in mechanical engineering from Seoul National University, Seoul, Korea, in 2011, where he is currently pursuing a combined Master's and doctorate degree in mechanical engineering.

His research interests are prognostics and health management and resilient system design.